



HAL
open science

HTLV-1 TRANSACTIVATOR TAX EXPLOITS THE XPB SUBUNIT OF TFIID DURING VIRAL TRANSCRIPTION

Christophe Martella, Armelle Inge Tollenaere, Laetitia Waast, Benoit Lacombe, Damien Groussaud, Florence Margottin-Goguet, Bertha Cecilia Ramirez, Claudine Pique

► **To cite this version:**

Christophe Martella, Armelle Inge Tollenaere, Laetitia Waast, Benoit Lacombe, Damien Groussaud, et al.. HTLV-1 TRANSACTIVATOR TAX EXPLOITS THE XPB SUBUNIT OF TFIID DURING VIRAL TRANSCRIPTION. *Journal of Virology*, 2020. hal-03020807

HAL Id: hal-03020807

<https://hal.science/hal-03020807>

Submitted on 24 Nov 2020

HAL is a multi-disciplinary open access archive for the deposit and dissemination of scientific research documents, whether they are published or not. The documents may come from teaching and research institutions in France or abroad, or from public or private research centers.

L'archive ouverte pluridisciplinaire **HAL**, est destinée au dépôt et à la diffusion de documents scientifiques de niveau recherche, publiés ou non, émanant des établissements d'enseignement et de recherche français ou étrangers, des laboratoires publics ou privés.

1 **HTLV-1 TRANSACTIVATOR TAX EXPLOITS THE XPB SUBUNIT OF TFIID**
2 **DURING VIRAL TRANSCRIPTION**

3 Christophe Martella ^{1,2,3}, Armelle Inge Tollenaere ^{1,2,3}, Laetitia Waast ^{1,2,3}, Benoit Lacombe
4 ^{1,2,3} Damien Groussaud ^{1,2,3}, Florence Margottin-Goguet ^{1,2,3}, Bertha Cecilia Ramirez ^{1,2,3,4} and
5 Claudine Pique ^{1,2,3*}

6
7 ¹ INSERM U1016, Retrovirus, Infection and Latency (RIL) Team, Institut Cochin, Paris,
8 France.

9 ² CNRS UMR8104, Paris, France.

10 ³ Université Paris Descartes, Université de Paris, Paris, France.

11 ⁴ Current address: Institute for Integrative Biology of the Cell, CNRS, Université Paris-
12 Saclay, CEA, Gif-Sur-Yvette, France.

13

14

15 * **Correspondence to:** Claudine Pique, email: claudine.pique@inserm.fr

16

17 **Keywords:** Retrovirus, oncoprotein, transcription, TFIID, promoter opening

18

19 **Short title:** XPB is a cofactor of HTLV-1 Tax

20 **ABSTRACT**

21 Human T-cell lymphotropic virus type 1 (HTLV-1) Tax oncoprotein is mandatory for viral
22 gene expression. Tax transactivates the viral promoter by recruiting specific transcription
23 factors but also by interfering with general transcription factors involved in the preinitiation
24 step, such as TBP, TFIIA and TFIID. However, data are lacking regarding Tax interplay with
25 TFIIH, which intervenes during the last step of preinitiation. We previously reported that
26 XPB, the TFIIH subunit responsible for promoter opening and promoter escape, is required
27 for Tat-induced Human-Immunodeficiency Virus promoter transactivation. Here, we
28 investigated whether XPB may also play a role in HTLV-1 transcription. We report that
29 endogenous XPB binds to Tax and is recruited on proviral LTR in HTLV-1-transformed T
30 cells but also in HTLV-1-immortalized primary T cells. In contrast, XPB recruitment at the
31 LTR is not detected in Tax-negative HTLV-1-infected T cells and is strongly reduced upon
32 Tax downregulation. XPB overexpression does not affect basal HTLV-1 promoter activation
33 but enhances Tax-mediated transactivation. Conversely, inducing XPB degradation strongly
34 reduces Tax-mediated transactivation. Importantly, this inhibition can be fully compensated
35 by overexpressing wild-type XPB but not a XPB mutant defective for the ATPase activity
36 responsible for promoter opening. Finally, XPB downregulation inhibits proliferation of Tax-
37 positive but not Tax-negative HTLV-1- T cell lines. These findings reveal that XPB is a novel
38 cellular co-factor hijacked by Tax to facilitate HTLV-1 transcription.

39 **IMPORTANCE**

40 HTLV-1 is considered the most potent human oncovirus and is also responsible for severe
41 inflammatory disorders. HTLV-1 transcription is taken in charge by RNA polymerase II and
42 is controlled by the viral oncoprotein Tax. Tax transactivates the viral promoter first *via* the
43 recruitment of CREB and its co-factors to the LTR. However, how Tax controls subsequent
44 steps of the transcription process remains unclear. In this study, we explore the link between

45 Tax and the XPB subunit of TFIID that governs, *via* its ATPase activity, the promoter
46 opening step of transcription. We demonstrate that XPB is a novel physical and functional
47 partner of Tax, recruited on the HTLV-1 LTR and required for viral transcription. These
48 findings extend the mechanism of Tax transactivation to the recruitment of TFIID and
49 reinforce the link between XPB and transactivator-induced viral transcription.

50

51

52

53

54

55

56

57

58

59

60 INTRODUCTION

61

62 Human T-lymphotropic virus type 1 (HTLV-1) is the etiologic agent of adult T-cell
63 leukemia/lymphoma (ATL), a very aggressive malignant proliferation of CD4+ T
64 lymphocytes (1, 2). In addition, HTLV-1 is also associated to various inflammatory disorders,
65 notably HTLV-1-associated myelopathy/tropical spastic paraparesis (HAM/TSP)(3).

66 The HTLV-1 genome encodes for structural, enzymatic, regulatory and auxiliary proteins.
67 Among them, the regulatory protein Tax is a major player for disease development (4, 5).
68 Indeed, Tax is an oncoprotein able to induce leukemia or lymphoma in transgenic mice (6) as
69 well as immortalization of primary human CD4+ T cells *in vitro* (7). Tax is also the
70 transactivator of the viral promoter located in the 5'LTR, thereby controlling its own
71 production as well as that of all sense HTLV-1 transcripts (8).

72 Transcription is an ordered process that proceeds through multiple stages including binding of
73 specific transcription factors to the promoter, assembly of the preinitiation complex (PIC),
74 promoter opening and escape, RNA polymerase II (Pol II) pausing, elongation and
75 termination (reviewed in (9, 10)). Tax controls the first step by recruiting the specific
76 transcription factor CREB at viral CREB-response elements (vCRE) located in the U3 region
77 of the 5'LTR (8, 11). This event was initially believed to be the only mechanism by which
78 Tax achieved maximal transcription. However, further data pointed towards additional key
79 roles of Tax on the subsequent steps of transcription (12). Indeed, Tax was also shown to
80 recruit to the LTR the general transcription factors (GTF) TBP (13), TFIIA (14), TFIID (15)
81 involved in PIC assembly as well as the elongation factor pTEF-b (16, 17). In contrast, data
82 are lacking regarding the specific involvement of TFIIH, which ensures transition between
83 preinitiation and elongation, in the context of Tax-dependent transcription.

84 TFIIH is a complex playing a dual role in DNA repair and transcription. It consists in five
85 non-enzymatic proteins, the CDK-activation kinase CAK (cyclin H, CDK7 and Mat1) and the
86 XPD and XPB enzymes (18). Within TFIIH, the ATPase and translocase *Xeroderma*
87 *Pigmentosum* type B (XPB) plays a key role in transcription (19). XPB acts as a molecular
88 wrench able to melt double stranded DNA, allowing opening and insertion of the sequence
89 around the transcription start into the active site of Pol II (19-22). The ATPase activity of
90 XPB is critical for the DNA opening while translocase activity is committed to promoter
91 escape (23-25). The ATPase activity of XPB is carried by the helicase domain 1 motif I and is
92 regulated by other regions of the protein, notably the helicase domain 1 R-E-D motif (24, 26,
93 27).

94 XPB plays a complex role in transcription that has only been clarified recently. Indeed,
95 Alekseev *et al.* demonstrated that XPB causes a regulatory block during preinitiation,
96 imposed by its translocase/helicase activity, then subsequently relieved by its own ATPase
97 activity (21, 28). Strikingly, this mechanism appears to be dispensable for basal transcription
98 while in contrast, transcription induced by trans-retinoic acid or cytokines was shown to be
99 sensitive to XPB downregulation (29, 30). This elucidation of XPB function has been greatly
100 facilitated by the use of a drug, Spironolactone (SP), originally described as an aldosterone
101 antagonist and later on identified as a compound able to induce rapid degradation of XPB
102 (30). Of note, ability to induce XPB degradation is not related to aldosterone signaling since
103 the SP derivative Eplerenone (EPL) antagonizes aldosterone signaling like SP but has no
104 impact on XPB (30). Strikingly, SP is believed to induce the degradation of XPB within
105 preformed TFIIH complexes, allowing XPB depletion while preserving TFIIH integrity (21,
106 30). A recent study showing that SP-induced XPB degradation depends on its prior
107 phosphorylation by CDK7 provides the molecular explanation for this selectivity (31).

108 In a previous study, we demonstrated that XPB is required for Tat-mediated human
109 immunodeficiency virus type 1 (HIV-1) promoter activation (32). This prompted us to
110 investigate the possibility that XPB could also contribute to HTLV-1 transcription. In this
111 study, we investigated the potential interaction between Tax and XPB as well as the impact of
112 XPB on HTLV-1 promoter transactivation and viral transcription.

113 **RESULTS**

114

115 **XPB binds to Tax**

116 Since Tax was previously shown to interact with certain GTFs, we examined whether it may
117 also interact with XPB. Co-immunoprecipitation experiments were first performed in 293T
118 cells cotransfected with an XPB-coding plasmid along or not with a Tax expressor or empty
119 vector. Immunoprecipitation of Tax allowed the recovery of XPB only in Tax cotransfected
120 cells (Fig. 1A, lane 4). The same experiment was repeated in C8166 T cells that endogenously
121 produce Tax and XPB. Immunoprecipitation with the anti-Tax antibody allowed the recovery
122 of XPB while only background signal was found upon precipitation with control IgG (Fig.
123 1B). Hence, XPB binds to Tax in both overexpression and endogenous conditions.

124

125 **XPB is recruited at proviral LTR in a Tax-dependent manner**

126 Whether XPB is recruited at the HTLV-1 LTR was examined by chromatin
127 immunoprecipitation (ChIP) experiments conducted in either Tax positive (C8166) or Tax
128 negative/low (TL-Om1, MT-1) HTLV-1-transformed T cell lines. TL-Om1 T cells do not
129 expressed Tax at either RNA or protein level (33) while MT-1 T cells were recently shown to
130 produce Tax protein only in a fraction of cells and in a transient manner (34). ChIP
131 experiments were also performed on CB-CD4/HTLV-1 T cells generated upon *in vitro*
132 activation of PBMC obtained from a HAM/TSP patient (35). Importantly, CB-CD4/HTLV-1
133 T cells remain dependent of exogenous IL-2 and present the same Tax or HBZ intracellular
134 distribution than fresh PBMC from HAM/TSP patients (36).

135 Following chromatin immunoprecipitation with a control (IgG) or anti-XPB antibody,
136 recovered DNA fragments were subjected to PCR using primers amplifying either the R or
137 U5 region of the LTR located downstream the transcription site start. The I κ B α (*NFKBIA*)

138 promoter region, at which XPB was shown to be recruited (29), was amplified as positive
139 control. In addition, the non-related α -satellite region was also amplified as negative control.
140 In both C8166 and CB-CD4/HTLV-1 T cells, XPB recruitment was observed at the R and U5
141 LTR regions (Fig. 2A). In contrast, no LTR-specific signal (R or U5 region) was detected for
142 either TL-Om1 or MT-1 T cells (Fig. 2B), strongly suggesting that XPB recruitment to the
143 LTR depends on Tax. ChIP experiments were validated by the fact that for all T cell lines,
144 positive XPB signals were found at the $\text{I}\kappa\text{B}\alpha$ promoter but not at the α -satellite region (Fig.
145 2A and 2B). Of note, Tax-negative HTLV-1-transformed T cells were shown to maintain
146 permanent NF- κ B activation despite the absence of Tax (37), explaining the positive XPB
147 signal found at the $\text{I}\kappa\text{B}\alpha$ promoter for both TL-Om1 and MT-1 T cells.

148 If Tax is required for XPB recruitment to the LTR, downregulating Tax expression should
149 lower the amount of XPB bound to the promoter. To address this hypothesis, we tried to
150 deplete Tax *via* siRNA in C8166 T cells but obtained only little decrease in global Tax level
151 (data not shown). Instead, we used chaetocin, an HSP90 inhibitor (38), since such inhibitors
152 were previously shown to induce rapid Tax degradation (39). Treating C8166 T cells with
153 chaetocin massively reduced Tax protein level without any effect on endogenous XPB (Fig.
154 2C). Tax downregulation coincided with a statistically significant reduction of the level of
155 XPB bound to the HTLV-1 LTR (Fig. 2D, left panel). In contrast, XPB was detected at the
156 same level at the $\text{I}\kappa\text{B}\alpha$ promoter (Fig. 2D, right panel), showing that chaetocin did not
157 prevent XPB recruitment at chromatin in a general manner.

158 Collectively, these findings strongly suggest that XPB is recruited on the HTLV-1 LTR in a
159 Tax-dependent manner.

160

161

162

163 **XPB is involved in Tax-mediated but not basal LTR activation**

164 To assess whether XPB recruitment at the viral promoter impacts LTR activation, luciferase
165 assays were performed in uninfected Jurkat T cells. We used an approach described by Elinoff
166 et al., based on XPB-overexpression in cells treated with SP in order to allow endogenous
167 XPB degradation (29). Eplerenone (EPL) was used as a control drug. Jurkat T cells were
168 transfected with the HTLV-1 LTR (U3R-Luc) reporter construct and pRL-TK normalization
169 plasmid together with a control (basal) or Tax (transactivation) plasmid and with or without
170 the XPB expressor, then treated with DMSO, EPL or SP for 24 hours. Neither SP treatment
171 nor XPB overexpression affected basal activation of the U3R-Luc construct (Fig. 3, upper
172 panel, bars 3 and 4), as compared to control cells (bar 1). In contrast, Tax-induced
173 transactivation was reduced by 50% in SP-treated cells as compared to DMSO-treated cells
174 (Fig. 3, upper panel, bars 7 and 9). The level of transfected Tax was similar in presence of
175 either DMSO or SP (Fig. 3, lower panel, lanes 7 and 9), indicating that SP influenced neither
176 Tax production from a CMV promoter nor Tax stability. Overexpressing XPB together with
177 Tax allowed to recover an XPB level close to the endogenous level (lanes 1 and 12), even
178 though overexpressed XPB was also partly sensitive to SP treatment (lanes 10 and 12). We
179 noticed that the level of intracellular XPB recovered upon XPB plasmid transfection was
180 higher in presence than in absence of Tax (lanes 6 and 12). This may be due to the ability of
181 Tax to transactivate the CMV promoter driving XPB expression, although higher XPB level
182 was not found in DMSO or EPL-treated Tax-transfected cells. Alternatively, this may indicate
183 that overexpressed Tax may somehow protects XPB from degradation triggered by SP.
184 Importantly, this XPB recovery fully reversed the inhibitory effect of SP on Tax-induced LTR
185 transactivation, independently on Tax level (Fig. 3, upper panel, bar 12).
186 These findings show that XPB is required for Tax-induced HTLV-1 LTR activation in T cells.
187 In addition, the rescue effect of XPB overexpression confirms that SP acts on promoter

188 activation in a XPB dependent manner, which validates SP as a relevant tool to analyze the
189 impact of XPB downregulation on transcription.

190

191 **The R-E-D domain of XPB is required for LTR transactivation and endogenous Tax**
192 **production**

193 To confirm that XPB is required for LTR transactivation by Tax, luciferase assays were
194 performed in C8166 T cells that produce Tax endogenously. In addition, we took advantage
195 of the ability of XPB to compensate SP-mediated XPB degradation to characterize the XPB
196 activity required for LTR transactivation. XPB contains various functional domains (25). In
197 particular, the R-E-D motif (Fig. 4A) was shown to be required for optimal ATPase activity
198 and promoter opening (26). We then used the XPB-E473A protein mutated in the R-E-D
199 region and two other XPB mutants retaining transcriptional activity but either defective
200 (F99S) or normal (T119P) for DNA repair activity (27). Importantly, the three mutants were
201 previously shown to be still properly incorporated within the TFIIH complex (26, 27).
202 Moreover, coimmunoprecipitation experiments performed in cotransfected 293T cells
203 demonstrated that each mutant remains capable of interacting with Tax (Fig. 4B).

204 Luciferase assays were then performed in HTLV-1-infected C8166 T cells transfected with
205 the reporter plasmids and one of the XPB construct in presence of DMSO, EPL or SP. As
206 expected, treating C8166 T cells with SP induced XPB downregulation, which coincided with
207 reduced production of endogenous Tax (Fig. 4C). In contrast, SP treatment did not affect the
208 production of phospho-CREB or that of specific protein 1 (Sp1), known to modulate Tax-
209 induced or basal LTR activation (40) (Fig. 4C). Strong reduction in LTR transactivation was
210 found in SP-treated control cells (Fig. 4D, upper panel, bar 3). Overexpressing wild-type (wt)
211 XPB, XPB-F99S or XPB-T119P reversed the effect of SP on LTR activation by Tax (Fig. 4D,
212 upper panel, bars 6, 9 and 12). In contrast, despite XPB-E473A was capable of increasing the

213 level of intracellular XPB like wt XPB and the two other mutants (Fig. 4D, lower panel, lane
214 15), this mutant was unable to rescue LTR transactivation in SP-treated cells (Fig. 4D, upper
215 panel, bar 15). Immunoblot analysis showed that overexpressing wt XPB, XPB-F99S or XPB-
216 T119P increased the level of endogenous Tax in SP-treated C8166 T cells (Fig. 4C, lower
217 panel, lanes 6, 9 and 12). In contrast, no such increase was observed for XPB-E473A (Fig.
218 4D, lower panel, compared lane 15 to lane 1).

219 These results show that XPB is involved in Tax-mediated LTR transactivation in the context
220 of integrated proviruses and further indicate that the R-E-D domain of XPB, regulating its
221 ATPase activity, is involved in this process.

222

223 **SP-mediated XPB downregulation inhibits viral transcription**

224 We next directly investigated the impact of XPB downregulation on HTLV-1 mRNA
225 production by RTqPCR experiments. C8166 and MT-4 HTLV-1-transformed T cells as well
226 as CB-CD4/HTLV-1-immortalized T cells were treated with DMSO, SP or EPL for 24 hours.
227 Of note, C8166 T cells exhibit a defect in viral RNA export and therefore do not produce Gag
228 proteins while they still produce Gag at the mRNA level (41). SP treatment inhibited the
229 production of Gag mRNA in C8166 (Fig. 5A), MT-4 (Fig. 5B, left panel) and HTLV-1-
230 immortalized CB-CD4/HTLV-1 (Fig. 5C, left panel) T cells. In both MT-4 and CB-
231 CD4/HTLV-1 T cells, this was accompanied by a reduction in Gag protein production (Fig.
232 5B and 5C, right panels).

233 To further study the link between HTLV-1 RNA production and XPB, we quantified the level
234 of HTLV-1 Gag mRNA in the course of SP treatment. C8166 T cells were treated with
235 DMSO, EPL or SP up to 6 hours. In agreement with previous data (30), XPB decrease can
236 already be seen 30 min post-treatment with a maximal reduction at 120 min (Fig. 5D).
237 Reduction of Gag mRNA began at 30 min (Fig. 5E, left panel), coinciding with the beginning

238 of XPB downregulation (Fig. 5D). Moreover, a solid positive correlation was found between
239 the level of Gag mRNA and the amount of XPB protein over the course of SP treatment (Fig.
240 5E, right panel). Importantly, no significant variation in the level of HPRT and EEF1G
241 housekeeping gene mRNAs was observed in the course of SP treatment (Fig. 5F), confirming
242 that SP does not act as a general inhibitor of Pol II-mediated transcription.

243

244 **SP-mediated XPB downregulation inhibits growth of Tax-positive HTLV-1-infected T** 245 **cells**

246 We finally studied the effect of XPB downregulation on the growth of HTLV-1-infected T
247 cells. Cells were treated every day with DMSO or with EPL or SP and the number of living
248 cells was quantified by the MTT method after 72h of culture. As compared to DMSO and
249 EPL, SP reduced the viability of C8166 (Fig. 6A) and MT-4 (Fig. 6B) T cells in a dose-
250 dependent manner. The same treatments were applied on Tax negative/low HTLV-1-infected
251 T cells (MT-1, TL-Om1) and uninfected T cells (Jurkat). Neither SP nor EPL impacted
252 viability of TL-Om1 (Fig. 6C) or Jurkat (Fig. 6E) T cells. Interestingly, SP at 10 μ M slightly
253 decreased viability of MT-1 T cells (Fig. 6D), in agreement with the transient expression of
254 Tax by this cell line (34). Importantly, SP treatment also reduced viability of CB-CD4/HTLV-
255 1 T cells in a dose-dependent manner (Fig. 6F), demonstrating that its cytotoxic effect also
256 applied on HTLV-1-immortalized primary T cells.

257 These data show that the effect of XPB downregulation on HTLV-1 RNA production
258 translates into inhibition of proliferation of Tax-positive HTLV-1-infected T cells, reinforcing
259 the link between Tax expression and XPB function.

260

261

262 **DISCUSSION**

263 As emphasized in recent reviews, HTLV-1 is considered the most potent cancer-associated
264 virus and still remains a significant threat to human health (42, 43). Deciphering the
265 mechanisms by which the HTLV-1 transactivator Tax regulates HTLV-1 gene expression is
266 therefore a central issue for both fundamental and therapeutic aspects. In this study, we
267 describe a novel physical and functional interaction between Tax and the XPB subunit of the
268 general transcription factor TFIID.

269 First, we found that Tax coprecipitates with XPB in cotransfected 293T cells as well as in
270 HTLV-1-infected T cells, in which the two proteins are produced endogenously. Second, we
271 showed that endogenous XPB is bound to the HTLV-1 LTR in Tax-positive but not Tax-
272 negative HTLV-1-transformed T cells, suggesting that XPB recruitment is mediated by Tax.
273 Importantly, XPB recruitment at the LTR was also observed in HTLV-1-immortalized T cells
274 generated from PBMC from an HAM/TSP patient. The role of Tax was confirmed by data
275 showing that inducing Tax degradation significantly reduced XPB recruitment at the LTR. Of
276 note, we checked that chaetocin treatment used to induce Tax degradation did not affect XPB
277 stability. Furthermore, chaetocin did not prevent XPB recruitment at a cellular promoter,
278 showing that XPB functionality was preserved. These data provide direct evidence that XPB
279 is a novel partner of Tax recruited by Tax at the LTR of integrated viral genomes in an
280 HTLV-1-transformed T cell line as well as in *in vivo*-infected T cells.

281 To assess the functional role of XPB, we next studied the impact of XPB overexpression on
282 HTLV-1 LTR activation using a reporter construct. We found that overexpressing XPB in
283 uninfected Jurkat T cells increases luciferase production only in presence of Tax, showing
284 that XPB is involved in Tax-induced but not basal LTR activation. Conversely, inducing XPB
285 degradation using the validated drug SP significantly reduces Tax-mediated LTR
286 transactivation in Jurkat T cells with no impact on Tax stability. SP-mediated XPB

287 downregulation also inhibits LTR transactivation mediated by endogenous Tax in HTLV-1-
288 transformed T cells, while the level of CREB or Sp1 was not affected. Of note, no significant
289 change in Tax-mediated LTR transactivation is observed upon treatment with EPL, arguing
290 against a role of aldosterone signaling modulation in LTR inhibition. The importance of XPB
291 is also attested by the fact that XPB overexpression is sufficient to reverse the negative effect
292 of SP on LTR transactivation in either Tax-transfected Jurkat T cells or HTLV-1-infected
293 C8166 T cells. This compensation effect gave us the opportunity to identify the domain of
294 XPB involved in Tax-mediated HTLV-1 transcription. Thus, we found that wild type XPB as
295 two XPB mutants defective for DNA repair but retaining transcriptional activity, fully
296 compensate SP-mediated XPB downregulation in C8166 T cells. In contrast, no compensation
297 is achieved with a mutant bearing a mutation in the R-E-D domain regulating XPB ATPase
298 activity (26). This strongly suggests that the ATPase-dependent activity of XPB, necessary for
299 the promoter opening activity, is indeed the one cooperating with Tax during HTLV-1
300 transcription.

301 Importantly, we also provide evidence that inducing XPB degradation had major
302 consequences on viral RNA expression and viability of HTLV-1-infected T cells. Indeed, we
303 showed that SP reduces the production of HTLV-1 Gag mRNA and that there is a solid
304 correlation between the level of Gag mRNA and the level of XPB. Moreover, we found that
305 as compared to EPL, SP inhibits the proliferation of HTLV-1-infected T cells. This was
306 observed in C8166 and MT-4 T cells but also in HTLV-1-immortalized CB-CD4/HTLV-1 T
307 cells, proving that the effect of XPB downregulation is not restricted to HTLV-1-transformed
308 T cells. In contrast, SP had no effect on either uninfected T cells or Tax-negative HTLV-1-
309 infected T cells. This reinforces the functional link between XPB and Tax and confirms the
310 key role of Tax in the survival of Tax-positive HTLV-1-infected T cells (44). These findings

311 also reveal that *via* its ability to downregulate XPB, SP is a potent inhibitor of Tax-induced
312 HTLV-1 gene expression as well as Tax-driven T cell proliferation.

313 Since XPB is member of a complex of general transcription factors, one could assume that its
314 downregulation would block transcription in a general manner. However, the role of XPB is
315 more complex. Indeed, while XPB appears to be dispensable for basal transcription, it is
316 required for transcription induced by certain stimuli. In good agreement with this, TFIIH was
317 shown to be at least partially dispensable in the case of promoters with preformed
318 transcription bubbles (45) while the promoter opening step, controlled by XPB, is considered
319 an important regulatory step for inducible promoters (46). We found here that SP-mediated
320 degradation of XPB impacts Tax-mediated but not basal HTLV-1-LTR activity in Jurkat T
321 cells. Noteworthy, we previously reported that SP inhibits Tat-dependent but not basal
322 transcription of the HIV-1 LTR (32). Our data therefore provide new evidence for a role of
323 XPB in inducible viral transcription by showing that XPB is also involved in HTLV-1 RNA
324 production.

325 Our demonstration that Tax interacts with XPB, raises the issue of whether XPB could also
326 directly interact with Tat to accomplish its function on the HIV-1 LTR promoter. In this line,
327 it would be also of interest to study the recruitment of XPB on the HIV-1 LTR sequence. Both
328 HIV-1 Tat (47) and HTLV-1 Tax (16) interact with pTEF-b but, in contrast to Tat, Tax is able
329 as well to recruit TFIIA and TFIID to the promoter. These findings, along with our present
330 data, support a model in which Tax not only recruits specific transcription factors to the
331 promoter but controls as well subsequent steps of the transcription process by successively
332 recruiting at least one subunit of each GTF complex acting together with RNA Pol II (Fig. 7).
333 This provides another example of the powerful ability of Tax to manipulate cellular
334 machineries.

335 In conclusion, this study demonstrates that XPB is a member of the Tax-dependent
336 transcription complexes assembled at the HTLV-1 LTR. Our data also suggest that the
337 promoter opening step of transcription plays a key role in HTLV-1 gene expression. These
338 findings provide new insights on the molecular players governing HTLV-1 transcription and
339 may open new avenues of research for the development of therapeutic interventions targeting
340 HTLV-1 transcription.

341 **MATERIALS AND METHODS**

342

343 **Cells and transfection**

344 HEK-293T (American Type Culture Collection CRL-3216) were grown in Dulbecco's
345 modified Eagle's medium supplemented with 10% fetal calf serum (Dutcher), 2 mM
346 glutamine, 1 mM pyruvate and antibiotics (Invitrogen) and were transfected using the
347 phosphate calcium procedure. Uninfected CD4+ Jurkat T-cells (kindly provided by S.
348 Emiliani, Institut Cochin, France) were grown in RPMI 1640 medium supplemented as above.
349 The HTLV-1-infected CD4+ T-cell lines C8166 and MT-4 (NIH AIDS Research and
350 Reference Reagent Program, USA), TL-Om1 and MT-1 (kindly provided by Dr. Harhaj, Johns
351 Hopkins School of Medicine, Baltimore, USA) were grown in supplemented RPMI 1640
352 containing also 25mM glucose, 20 mM HEPES and 5mL of 100X non-essential aminoacid
353 solution (Invitrogen). T cell lines were transfected using the DMRIE-C reagent (Roche).
354 HTLV-1-immortalized CB-CD4/HTLV-1 T cells generated from peripheral blood
355 mononuclear cells of a TSP/HAM patient have been described in (35). These cells were
356 grown in supplemented RPMI medium in the presence of 50U/ml of IL-2 (Roche, France).

357 **Plasmids**

358 The pSG5M empty vector and pSG5M-Tax plasmids were described elsewhere (48). The
359 U3R-Luc (Firefly) plasmid was kindly provided by A. Kress (Germany). The normalization
360 plasmid pRL-TK (Renilla) was obtained from Promega. Human XPB cDNA was cloned from
361 total RNA extracted from Jurkat T cells by using the RNeasy Mini Kit (Qiagen). One µg of
362 total RNA was subjected to reverse transcription using the Maxima Reverse Transcriptase
363 (Thermo Fisher Scientific). PCR amplification was performed on a fraction of RT products
364 with the high fidelity Platinum Taq DNA Polymerase (Invitrogen) using the oligonucleotides

365 XPB-BamHI Fw (5' GCGCCTCGAGGATCCACCATGGGCAAAAGAGACCGAGGC 3') and
366 XPB NheI Rev (5' GCGCACGCGTGC GGCCGCTAGCTCATTTCCTAAAGCGCTTGAAG 3')
367 and products were then cloned in the pCR-Blunt II-TOPO vector (Invitrogen). The XPB insert
368 was then digested with BamHI and NheI and cloned into the pcDNA3 vector (Invitrogen).
369 XPB mutagenesis was performed on the pcDNA3-XPB plasmid by PCR amplification with
370 the high fidelity proof reading Pfu Turbo DNA Polymerase (Stratagene) using the following
371 primers: F99S (Fw: 5' CAAATATGCCCAAGACTCCTTGGTGGCTATTGC 3', F99S Rev: 5'
372 GCAATAGCCACCAAGGAGTCTTGGGCATATTTG 3); T119P (Fw: 5'CATGAGTACAAACTA
373 CCTGCCTACTCCTTG 3', T119P Rev: 5' CAAGGAGTAGGCAGGTAGTTTGTACTCATG 3');
374 K346R (Fw: 5' CCCTGCGGTGCTGGAAGGTCCCTGGTTGGTGTC 3', K346R Rev:
375 5'CACACCAACGGGACCTTCCAGCACCGCAGGG 3'); E473A (Fw: 5'GCGACCCTCGTCCGCG
376 CAATGACAAAATTGTG 3', E473A Rev: 5'CACAATTTTGTTCATCTGCGCGGA CGAGGGTCGC
377 3'). Sequencing of the wt and mutated plasmids showed that the XPB ORF was identical in
378 each cDNA excepted for the presence of the introduced mutation.

379

380 **Antibodies and reagents**

381 The anti XPB monoclonal antibody from Novusbio (NB10061060) was used for ChIP
382 experiment. The following other primary antibodies were used in immunoblots: anti-XPB
383 (Santa Cruz, s19), anti-pCREB-Ser133 (Millipore, CS 204400), anti-Sp1 (Abcam ab13370),
384 anti-GAPDH (Santa Cruz, sc32233), anti-gammatubulin (Abcam ab16504), anti-lamin A/C
385 (Cell signaling, 2032S) and anti-IgG rabbit (Millipore PP64B). HRP-conjugated anti-human,
386 anti-mouse and anti-rabbit IgG (Promega) were used as secondary antibodies. Spironolactone
387 (SP), Eplerenone (EPL) and Chaetocin (all from Sigma) were diluted in dimethyl sulfoxide
388 (DMSO) as 10 mM stock solutions.

389

390

391 **Luciferase assays**

392 T cells (3×10^5 /24 well in duplicate) were cotransfected using the DMRIE-C reagent (Roche)
393 with 100 ng of the U3R-Luc plasmid, 10 ng of pRL-TK and 250 ng of the control, Tax or
394 XPB plasmid/well. After 48 hours, cells were lysed in 100 μ L of Passive lysis buffer
395 (Promega). Luciferase activities were quantified using the Dual Luciferase Assay System
396 (Promega) and Firefly activity values were normalized to that of Renilla activity.

397

398 **Immunoprecipitation and immunoblot**

399 293T cells (1.5×10^6 cells in 10 cm dish) were transfected with 6 μ g of the control, Tax or XPB
400 plasmid and lysed 48h post-transfection. Transfected 293T cells or C8166 T cells (5×10^6)
401 were lysed in 500 μ L of RIPA buffer (50 mM Tris-HCl pH8, 1% NP40, 0.5% deoxycholate,
402 0.1% SDS and 150 mM NaCl) supplemented with protease inhibitor and benzonase nuclease
403 (Sigma). 500 μ g of the lysates were incubated overnight with 3 μ g of primary antibodies at 4°C
404 and 10 μ g of the lysates were used for western blot analysis. Immunocomplexes were then
405 captured on protein A/G-agarose beads (Thermoscientific 20421) 1h at 4°C. Sepharose beads
406 were then washed 5 times in wash buffer (120 mM NaCl, 20mM Tris-HCl pH8, 0.2 mM NaF,
407 0.2 mM EGTA, 0.2% deoxycholate, 0.5% NP40) before elution in 50 μ L of Laemmli buffer
408 (0.3 M Tris-HCl pH6.8, 10% SDS, 20% Glycerol, 0.04% Bromophenol Blue, DTT 100 mM).
409 Immunoprecipitated proteins or total cell lysates were separated on 4-15% SDS-PAGE,
410 transferred to nitrocellulose membranes (0.45 μ m) and blotted with specific antibodies.
411 Images were acquired using a Fusion Fx camera (Vilber Lourmat). Band quantification was
412 performed with the Image J software after subtraction of the background.

413

414 **RNA extraction and RT-qPCR**

415 Total RNAs were prepared with the Nucleospin RNAII kit (Macherey Nagel, France) and 1 μ g

416 was reverse-transcribed using the Maxima first strand cDNA synthesis kit (Thermo Scientific,
417 France). Real-time PCR were performed on 1/10 of the reverse transcription reaction. HTLV-
418 1 genomic RNA (gRNA) and housekeeping control RNAs were amplified using the Sybr
419 Green method with the following primers: unspliced Gag mRNA (region 2036 to 2224, Fw
420 5'CAGAGGAAGATGCCCTCCTATT 3', Rev: 5' GTCAACCTGGGCTTTAATTACG 3');
421 Total sense RNA (Fw: TTCCCAGGGTTTGGACAGAG, Rev:
422 GATGGGGTCCCAGGTGATCT); EEF1G (Fw: AGATGGCCCAGTTTGATGCTAA, Rev:
423 GCTTCTCTTCCCGTGAACCCT), HPRT (Fw: TGACACTGGCAAACAATGCA, Rev:
424 GGTCCTTTTCACCAGCAAGCT). PCR conditions were as followed: pre-incubation 95° 5
425 min x1; amplification x45: denaturation 95° 10 sec; annealing 60° 20 sec; extension 72° 10
426 sec; acquisition, melting curve, cooling. The normalized quantity (NQ) of each mRNA was
427 determined by normalizing their level to that of the housekeeping genes EEF1G and HPRT
428 according to the following formula: $NQ=2^{-(cp-((cpEEF1G+cpHPRT)/2))}$.

429

430 **CHIP experiments**

431 Before the experiment, 10^7 cells were crosslinked using 1.1% Formaldehyde (Electron
432 Microscopy Sciences) for 8 minutes at room temperature. Chromatin was then sheared using a
433 Bioruptor Pico sonicator to obtain fragments of approximately 300 bp. IP were performed
434 using the ChIP-IT high sensitivity kit (Active motif) on 10 µg of chromatin using 4 µg of
435 specific or control antibodies and 10% of chromatin was kept for inputs. qPCR were
436 conducted with the following primers: a-sat (Fw: CTGCACTACCTGAAGAGGAC, Rev:
437 GATGGTTCAACTCTTACA), IκBα (SimpleChIP® Human IκBα Promoter Primers
438 #5552, Cell Signaling Technology), LTR R region (Fw: CGCATCTCTCCTTCACGCGC,
439 Rev: CGGTCTCGACCTGAG) or LTR U5 region (Fw: GACAGCCCATCCTATAGCACTC,
440 Rev: CTAGCGCTACGGGAAAAGATT).

441 **Cell viability assay**

442 Cell viability was quantified by measuring the rate of mitochondrial reduction of yellow
443 tetrazolium salt MTT (3-(4,5-dimethylthiazol-2-yl)-2,5-diphenyltetrazolium bromide (Sigma)
444 to insoluble purple crystals. Cells were cultivated for 72h with DMSO, EPL or SP and MTT
445 solution (25 μ L of a solution at 5 mg/mL) was added to each well for 2 hours. The supernatant
446 was then removed and 50 μ L of DMSO added to dissolve formazan crystal. Optical densities
447 (OD) were measured at 590 nm with a Tecan infinite Pro 2000 spectrophotometer.

448

449 **Statistical analysis**

450 Statistical analyses were conducted with the GraphPad Prism 6 software. Two-group
451 comparison was done using the paired t test and multiple-group analysis with the one-way
452 ANOVA Tukey's multiple comparisons test. Correlation analysis was done using the Pearson
453 test. Statistical significance was defined for p-values < 0.05 .

454 **ACKNOWLEDGMENTS**

455

456 We thank the AIDS Research and Reference Reagent Program, Division of AIDS, NIAID,
457 NIH, for the HTLV-1 infected T-cell lines. We also thank the staff of the Genomic core
458 facilities of the Cochin Institute for their expertise in RTqPCR.

459 This work was supported by grants from the Ligue contre le Cancer (Comité Ile de France,
460 [url:https://www.ligue-cancer.net/cd75](https://www.ligue-cancer.net/cd75)) and from Fondation pour la Recherche Médicale
461 (FRM, grant number DEQ20140329528 attributed to FMG, [url:https://www.frm.org/](https://www.frm.org/)). CM
462 and AT were recipients of PhD grants from the Ligue Nationale contre le Cancer ([url:](https://www.ligue-cancer.net)
463 <https://www.ligue-cancer.net>) or from Université Paris Descartes ([url:](https://www.parisdescartes.fr/)
464 <https://www.parisdescartes.fr/>) and Fondation ARC ([url: https://www.fondationarc.org/](https://www.fondationarc.org/)),
465 respectively. The funders had no role in study design, data collection and interpretation, or the
466 decision to submit the work for publication.

467

468 **FIGURE LEGENDS**

469

470 **Figure 1. XPB binds to Tax.**

471 (A) Coprecipitation of Tax and XPB in cotransfected 293T cells. Total proteins prepared 24
472 hours post-transfection were analyzed by immunoblot before (Lysates) or after anti-Tax
473 immunoprecipitation (IP Tax). Data correspond to one representative experiment out of two.
474 (B) Coprecipitation of endogenous Tax and XPB produced in HTLV-1-transformed C8166 T
475 cells. Immunoprecipitated proteins (IP Tax, left panel) or total proteins obtained before
476 (input) or after (flowthrough) IP (right panels) were analyzed by immunoblot. Data
477 correspond to one representative experiment out of two. Ig: signal corresponding to
478 immunoglobulins used for the IP.

479

480 **Figure 2. Endogenous XPB is recruited at proviral LTR in a Tax-dependent manner**

481 (A,B) ChIP experiments to detect XPB recruitment at various genomic loci. Sonicated
482 chromatin prepared for (A) Tax-positive C8166 and CB-CD4/HTLV-1 or (B) Tax-
483 negative/low MT-1 and TL-Om1 HTLV-1-infected T cells were used before (input) or after
484 immunoprecipitation with control IgG or the anti-XPB antibody. PCR reactions were then
485 performed using primers specific for the R or U5 region of the HTLV-1 LTR or for the $\text{I}\kappa\text{B}\alpha$
486 promoter (positive control) and the α -satellite regions (negative control). PCR amplification
487 gave positive signals for both R and U5 regions in the four T cell lines (18 to 22 PCR cycles
488 as compared to 37 to 45 for water), confirming that they all carried integrated HTLV-1
489 genomes. Data correspond to means \pm SEM of two independent experiments performed in
490 triplicate. (C) Effect of Tax downregulation on XPB recruitment to the HTLV-1 promoter.
491 C8166 T cells were treated with 100 nM of chaetocin for 24 hours. Left panel shows the
492 effect of chaetocin on the levels of endogenous Tax and XPB analyzed by immunoblot (one

493 representative experiment out of two). **(D)** Effect of chaetocin treatment on XPB recruitment
494 to either the LTR or the $\text{I}\kappa\text{B}\alpha$ promoter. CHIP analysis was performed as in (A). Data
495 correspond to means \pm SEM of one experiment performed in triplicate out of 2. Statistical
496 significance: ns: not significant, *: $p < 0.05$, **: $p < 0.01$, ***: $p < 0.001$, *****: $p < 0.0001$.

497

498 **Figure 3. XPB is involved in Tax-mediated but not basal HTLV-1 LTR activation**

499 Effect of XPB overexpression on HTLV-1 LTR activation in Jurkat T cells. Cells were
500 transfected with the LTR U3R-Luc and pRL-TK reporter plasmids along with control (basal),
501 Tax (transactivation) or the XPB plasmid and then treated with DMSO or with EPL or SP at
502 10 μM for 24 hours. Upper panel: relative luciferase activity calculated by normalizing
503 Firefly/Renilla ratios to that of DMSO-treated Tax-transfected cells (set to 1). Data are means
504 \pm SEM of three independent experiments performed in duplicate. Lower panel: Tax and XPB
505 expression levels detected by immunoblot. Data are from one representative experiment out of
506 two. Statistical significance: *: $p < 0.05$, **: $p < 0.01$.

507

508 **Figure 4. The R-E-D domain of XPB is required for LTR transactivation and** 509 **endogenous Tax production**

510 **(A)** Schematic representation of the XPB protein and position of the XPB mutations. **(B)**
511 Interaction of Tax with wild type XPB or XPB mutants. 293T cells were cotransfected with
512 one of the XPB constructs along with a control or Tax expressor. Total proteins prepared 24
513 hours post-transfection were separated before (lysates) or after the anti-Tax
514 immunoprecipitation (IP Tax). Data correspond to one representative experiment out of two.
515 **(C)** Immunoblots performed in HTLV-1-transformed C8166 T cells to analyze expression
516 levels of XPB, Tax, phospho-CREB (Ser133) and Specific factor 1 (Sp1) upon SP treatment.
517 **(D)** Capacity of wt or mutated XPB proteins to rescue SP-mediated inhibition of either LTR

518 transactivation or endogenous Tax production. HTLV-1-transformed C8166 T cells were
519 transfected with the LTR U3R-Luc and pRL-TK reporter plasmids and one of the XPB
520 construct and were then treated with DMSO or with EPL or SP at 10 μ M for 48 hours. Upper
521 panel: relative luciferase activity calculated by normalizing Firefly/Renilla ratios to that of
522 DMSO-treated control cells (set to 1). Data are means \pm SEM of five independent
523 experiments performed in duplicate. Lower panel: Tax and XPB expression levels detected by
524 immunoblot. Data are from one representative experiment out of three. Statistical
525 significance: ns: not significant, ****: $p < 0.0001$.

526

527 **Figure 5. XPB downregulation inhibits viral transcription**

528 (A) C8166 and (B) MT-4 HTLV-1-transformed T cells or (C) HTLV-1-immortalized CB-
529 CD4/HTLV-1 T cells were treated with DMSO or with SP or EPL at 10 μ M for 24 hours. The
530 level of unspliced Gag mRNA was quantified by RTqPCR and normalized to the level of
531 housekeeping genes (left panels). For MT-4 and CB-CD4/HTLV-1 T cells, the level of Gag
532 protein (p19) was also analyzed by immunoblot (right panels). Data correspond to one
533 representative experiment out of two or three. (D-F) Time-course experiment to quantify the
534 level of Gag mRNA over the course of SP treatment. C8166 T cells were either untreated
535 (NT) or treated with DMSO or with SP or EPL at 10 μ M. (D) The level of XPB was analyzed
536 at indicated times by immunoblot in half of the cells. At each time-point, the intensity of the
537 XPB signal in EPL or SP-treated cells was compared to that of DMSO-treated cells (set to 1).
538 Data correspond to one representative experiment out of three. (E) The other half of the cells
539 was used to quantify the level of Gag mRNA. Left panel shows the SP/DMSO ratios
540 calculated from the level of RNA normalized to the level of housekeeping genes (NQ). Right
541 panel shows correlation between the level of XPB protein quantified from (A) and the
542 SP/DMSO ratios shown in the left panel. (F) Effect of SP on the levels of housekeeping gene

543 mRNAs. Data show the SP/DMSO ratios for HPRT or EEF1G calculated from relative
544 quantities using the formula: $Q=2^{-C_p}$. Data correspond to one representative experiment
545 performed in triplicate out of 3.

546

547 **Figure 6. XPB downregulation reduces viability of Tax-positive HTLV-1-infected T**
548 **cells.**

549 (A) C8166, (B) MT-4, (C) TL-om1, (D) MT-1 and (E) Jurkat transformed T cells or (F)
550 HTLV-1 immortalized CB-CD4/HTLV-1 were treated every day with DMSO (0) or with EPL
551 or SP at indicated concentrations and cell viability was determined by the MTT method after
552 3 days of culture. The viability values for SP or EPL were normalized to that of DMSO-
553 treated cells (set as 100%). For each cell line, viability results correspond to two independent
554 experiments performed in triplicate. Ns: not significant, *: $p<0.05$, **: $p<0.01$; ***: $p<0.001$,
555 ****: $p<0.0001$.

556

557 **Figure 7. Model illustrating the capacity of Tax to target essential steps of the Pol II-mediated**
558 **transcription process, including the promoter opening step controlled by the XPB subunit of**
559 **TFIIH.**

560

561

562

563

564

565 **REFERENCES**

- 566 1. Hermine O, Ramos JC, Tobinai K. 2018. A Review of New Findings in Adult T-cell
567 Leukemia-Lymphoma: A Focus on Current and Emerging Treatment Strategies. *Adv*
568 *Ther* 35:135-152.
- 569 2. Panfil AR, Martinez MP, Ratner L, Green PL. 2016. Human T-cell leukemia virus-
570 associated malignancy. *Curr Opin Virol* 20:40-46.
- 571 3. Bangham CR, Araujo A, Yamano Y, Taylor GP. 2015. HTLV-1-associated
572 myelopathy/tropical spastic paraparesis. *Nat Rev Dis Primers* 1:15012.
- 573 4. Curren R, Van Duyne R, Jaworski E, Guendel I, Sampey G, Das R, Narayanan A,
574 Kashanchi F. 2012. HTLV tax: a fascinating multifunctional co-regulator of viral and
575 cellular pathways. *Front Microbiol* 3:406.
- 576 5. Kfoury Y, Nasr R, Journo C, Mahieux R, Pique C, Bazarbachi A. 2012. The
577 multifaceted oncoprotein Tax: subcellular localization, posttranslational modifications,
578 and NF-kappaB activation. *Adv Cancer Res* 113:85-120.
- 579 6. Hasegawa H, Sawa H, Lewis MJ, Orba Y, Sheehy N, Yamamoto Y, Ichinohe T,
580 Tsunetsugu-Yokota Y, Katano H, Takahashi H, Matsuda J, Sata T, Kurata T,
581 Nagashima K, Hall WW. 2006. Thymus-derived leukemia-lymphoma in mice
582 transgenic for the Tax gene of human T-lymphotropic virus type I. *Nat Med* 12:466-
583 72.
- 584 7. Bellon M, Baydoun HH, Yao Y, Nicot C. 2010. HTLV-I Tax-dependent and -
585 independent events associated with immortalization of human primary T lymphocytes.
586 *Blood* 115:2441-8.
- 587 8. Nyborg JK, Egan D, Sharma N. 2010. The HTLV-1 Tax protein: revealing
588 mechanisms of transcriptional activation through histone acetylation and nucleosome
589 disassembly. *Biochim Biophys Acta* 1799:266-74.

- 590 9. Chen FX, Smith ER, Shilatifard A. 2018. Born to run: control of transcription
591 elongation by RNA polymerase II. *Nat Rev Mol Cell Biol* 19:464-478.
- 592 10. Nogales E, Louder RK, He Y. 2017. Structural Insights into the Eukaryotic
593 Transcription Initiation Machinery. *Annu Rev Biophys* 46:59-83.
- 594 11. Lemasson I, Polakowski NJ, Laybourn PJ, Nyborg JK. 2002. Transcription factor
595 binding and histone modifications on the integrated proviral promoter in human T-cell
596 leukemia virus-I-infected T-cells. *J Biol Chem* 277:49459-65.
- 597 12. de la Fuente C, Kashanchi F. 2004. The expanding role of Tax in transcription.
598 *Retrovirology* 1:19.
- 599 13. Caron C, Rousset R, Beraud C, Moncollin V, Egly JM, Jalinot P. 1993. Functional and
600 biochemical interaction of the HTLV-I Tax1 transactivator with TBP. *EMBO J*
601 12:4269-78.
- 602 14. Clemens KE, Piras G, Radonovich MF, Choi KS, Duvall JF, DeJong J, Roeder R,
603 Brady JN. 1996. Interaction of the human T-cell lymphotropic virus type 1 tax
604 transactivator with transcription factor IIA. *Mol Cell Biol* 16:4656-64.
- 605 15. Anderson MG, Scoggin KE, Simbulan-Rosenthal CM, Steadman JA. 2000.
606 Identification of poly(ADP-ribose) polymerase as a transcriptional coactivator of the
607 human T-cell leukemia virus type 1 Tax protein. *J Virol* 74:2169-77.
- 608 16. Zhou M, Lu H, Park H, Wilson-Chiru J, Linton R, Brady JN. 2006. Tax interacts with
609 P-TEFb in a novel manner to stimulate human T-lymphotropic virus type 1
610 transcription. *J Virol* 80:4781-91.
- 611 17. Cho WK, Zhou M, Jang MK, Huang K, Jeong SJ, Ozato K, Brady JN. 2007.
612 Modulation of the Brd4/P-TEFb interaction by the human T-lymphotropic virus type 1
613 tax protein. *J Virol* 81:11179-86.

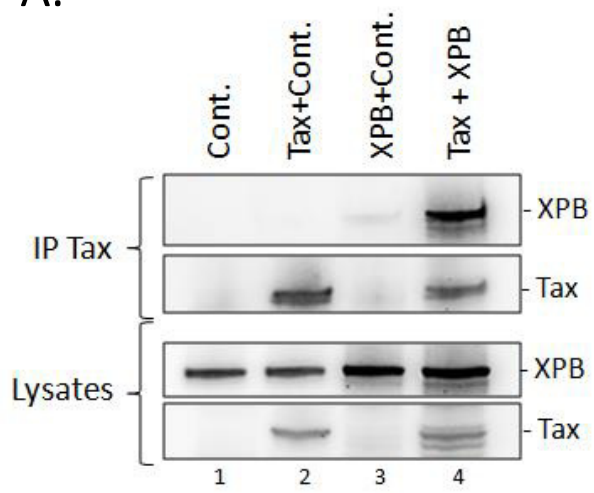
- 614 18. Rimel JK, Taatjes DJ. 2018. The essential and multifunctional TFIIH complex. *Protein*
615 *Sci* 27:1018-1037.
- 616 19. Compe E, Egly JM. 2016. Nucleotide Excision Repair and Transcriptional Regulation:
617 TFIIH and Beyond. *Annu Rev Biochem* 85:265-90.
- 618 20. Fishburn J, Tomko E, Galburt E, Hahn S. 2015. Double-stranded DNA translocase
619 activity of transcription factor TFIIH and the mechanism of RNA polymerase II open
620 complex formation. *Proc Natl Acad Sci U S A* 112:3961-6.
- 621 21. Alekseev S, Nagy Z, Sandoz J, Weiss A, Egly JM, Le May N, Coin F. 2017.
622 Transcription without XPB Establishes a Unified Helicase-Independent Mechanism of
623 Promoter Opening in Eukaryotic Gene Expression. *Mol Cell* 65:504-514 e4.
- 624 22. Kim TK, Ebright RH, Reinberg D. 2000. Mechanism of ATP-dependent promoter
625 melting by transcription factor IIH. *Science* 288:1418-22.
- 626 23. Tirode F, Busso D, Coin F, Egly JM. 1999. Reconstitution of the transcription factor
627 TFIIH: assignment of functions for the three enzymatic subunits, XPB, XPD, and
628 cdk7. *Mol Cell* 3:87-95.
- 629 24. Lin YC, Choi WS, Gralla JD. 2005. TFIIH XPB mutants suggest a unified bacterial-
630 like mechanism for promoter opening but not escape. *Nat Struct Mol Biol* 12:603-7.
- 631 25. Oksenyich V, Coin F. 2010. The long unwinding road: XPB and XPD helicases in
632 damaged DNA opening. *Cell Cycle* 9:90-6.
- 633 26. Oksenyich V, Bernardes de Jesus B, Zhovmer A, Egly JM, Coin F. 2009. Molecular
634 insights into the recruitment of TFIIH to sites of DNA damage. *EMBO J* 28:2971-80.
- 635 27. Coin F, Oksenyich V, Egly JM. 2007. Distinct roles for the XPB/p52 and XPD/p44
636 subcomplexes of TFIIH in damaged DNA opening during nucleotide excision repair.
637 *Mol Cell* 26:245-56.

- 638 28. Sandoz J, Coin F. 2017. Unified promoter opening steps in eukaryotic gene
639 expression. *Oncotarget* 8:84614-84615.
- 640 29. Elinoff JM, Chen LY, Dougherty EJ, Awad KS, Wang S, Biancotto A, Siddiqui AH,
641 Weir NA, Cai R, Sun J, Preston IR, Solomon MA, Danner RL. 2018. Spironolactone-
642 induced degradation of the TFIID core complex XPD subunit suppresses NF-kappaB
643 and AP-1 signalling. *Cardiovasc Res* 114:65-76.
- 644 30. Alekseev S, Ayadi M, Brino L, Egly JM, Larsen AK, Coin F. 2014. A small molecule
645 screen identifies an inhibitor of DNA repair inducing the degradation of TFIID and the
646 chemosensitization of tumor cells to platinum. *Chem Biol* 21:398-407.
- 647 31. Ueda M, Matsuura K, Kawai H, Wakasugi M, Matsunaga T. 2019. Spironolactone-
648 induced XPD degradation depends on CDK7 kinase and SCF(FBXL) (18) E3 ligase.
649 *Genes Cells* doi:10.1111/gtc.12674.
- 650 32. Lacombe B, Morel M, Margottin-Goguet F, Ramirez BC. 2016. Specific Inhibition of
651 HIV Infection by the Action of Spironolactone in T Cells. *J Virol* 90:10972-10980.
- 652 33. Hironaka N, Mochida K, Mori N, Maeda M, Yamamoto N, Yamaoka S. 2004. Tax-
653 independent constitutive IkappaB kinase activation in adult T-cell leukemia cells.
654 *Neoplasia* 6:266-78.
- 655 34. Mahgoub M, Yasunaga JI, Iwami S, Nakaoka S, Koizumi Y, Shimura K, Matsuoka M.
656 2018. Sporadic on/off switching of HTLV-1 Tax expression is crucial to maintain the
657 whole population of virus-induced leukemic cells. *Proc Natl Acad Sci U S A*
658 115:E1269-E1278.
- 659 35. Ozden S, Cochet M, Mikol J, Teixeira A, Gessain A, Pique C. 2004. Direct evidence
660 for a chronic CD8+-T-cell-mediated immune reaction to tax within the muscle of a
661 human T-cell leukemia/lymphoma virus type 1-infected patient with sporadic
662 inclusion body myositis. *J Virol* 78:10320-7.

- 663 36. Forlani G, Baratella M, Tedeschi A, Pique C, Jacobson S, Accolla RS. 2019. HTLV-1
664 HBZ Protein Resides Exclusively in the Cytoplasm of Infected Cells in Asymptomatic
665 Carriers and HAM/TSP Patients. *Front Microbiol* 10:819.
- 666 37. Mori N, Fujii M, Ikeda S, Yamada Y, Tomonaga M, Ballard DW, Yamamoto N. 1999.
667 Constitutive activation of NF-kappaB in primary adult T-cell leukemia cells. *Blood*
668 93:2360-8.
- 669 38. Song X, Zhao Z, Qi X, Tang S, Wang Q, Zhu T, Gu Q, Liu M, Li J. 2015.
670 Identification of epipolythiodioxopiperazines HDN-1 and chaetocin as novel inhibitor
671 of heat shock protein 90. *Oncotarget* 6:5263-74.
- 672 39. Gao L, Harhaj EW. 2013. HSP90 protects the human T-cell leukemia virus type 1
673 (HTLV-1) tax oncoprotein from proteasomal degradation to support NF-kappaB
674 activation and HTLV-1 replication. *J Virol* 87:13640-54.
- 675 40. Yao J, Grant C, Harhaj E, Nonnemacher M, Alefantis T, Martin J, Jain P, Wigdahl B.
676 2006. Regulation of human T-cell leukemia virus type 1 gene expression by Sp1 and
677 Sp3 interaction with TRE-1 repeat III. *DNA Cell Biol* 25:262-76.
- 678 41. Bhat NK, Adachi Y, Samuel KP, Derse D. 1993. HTLV-1 gene expression by
679 defective proviruses in an infected T-cell line. *Virology* 196:15-24.
- 680 42. Martin F, Tagaya Y, Gallo R. 2018. Time to eradicate HTLV-1: an open letter to
681 WHO. *Lancet* 391:1893-1894.
- 682 43. Tagaya Y, Gallo RC. 2017. The Exceptional Oncogenicity of HTLV-1. *Front*
683 *Microbiol* 8:1425.
- 684 44. Dassouki Z, Sahin U, El Hajj H, Jollivet F, Kfoury Y, Lallemand-Breitenbach V,
685 Hermine O, de The H, Bazarbachi A. 2015. ATL response to arsenic/interferon
686 therapy is triggered by SUMO/PML/RNF4-dependent Tax degradation. *Blood*
687 125:474-82.

- 688 45. Hahn S. 2004. Structure and mechanism of the RNA polymerase II transcription
689 machinery. *Nat Struct Mol Biol* 11:394-403.
- 690 46. Kouzine F, Wojtowicz D, Yamane A, Resch W, Kieffer-Kwon KR, Bandle R, Nelson
691 S, Nakahashi H, Awasthi P, Feigenbaum L, Menoni H, Hoeijmakers J, Vermeulen W,
692 Ge H, Przytycka TM, Levens D, Casellas R. 2013. Global regulation of promoter
693 melting in naive lymphocytes. *Cell* 153:988-99.
- 694 47. Rice AP. 2017. The HIV-1 Tat Protein: Mechanism of Action and Target for HIV-1
695 Cure Strategies. *Curr Pharm Des* 23:4098-4102.
- 696 48. Nasr R, Chiari E, El-Sabban M, Mahieux R, Kfoury Y, Abdulhay M, Yazbeck V,
697 Hermine O, de The H, Pique C, Bazarbachi A. 2006. Tax ubiquitylation and
698 sumoylation control critical cytoplasmic and nuclear steps of NF-kappaB activation.
699 *Blood* 107:4021-9.
- 700

A.



B.

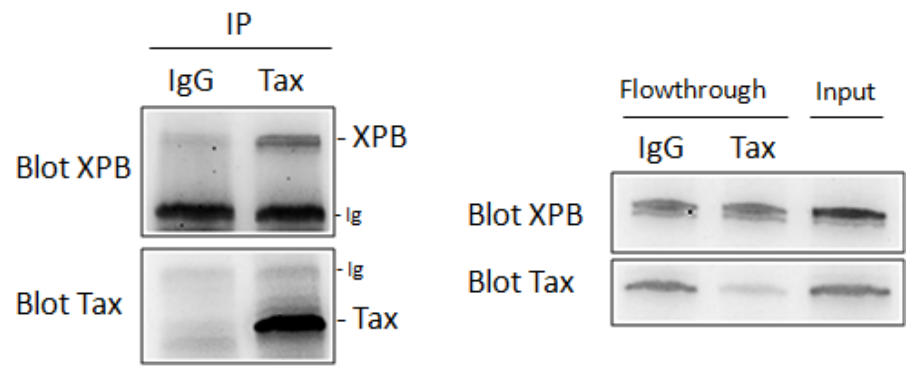
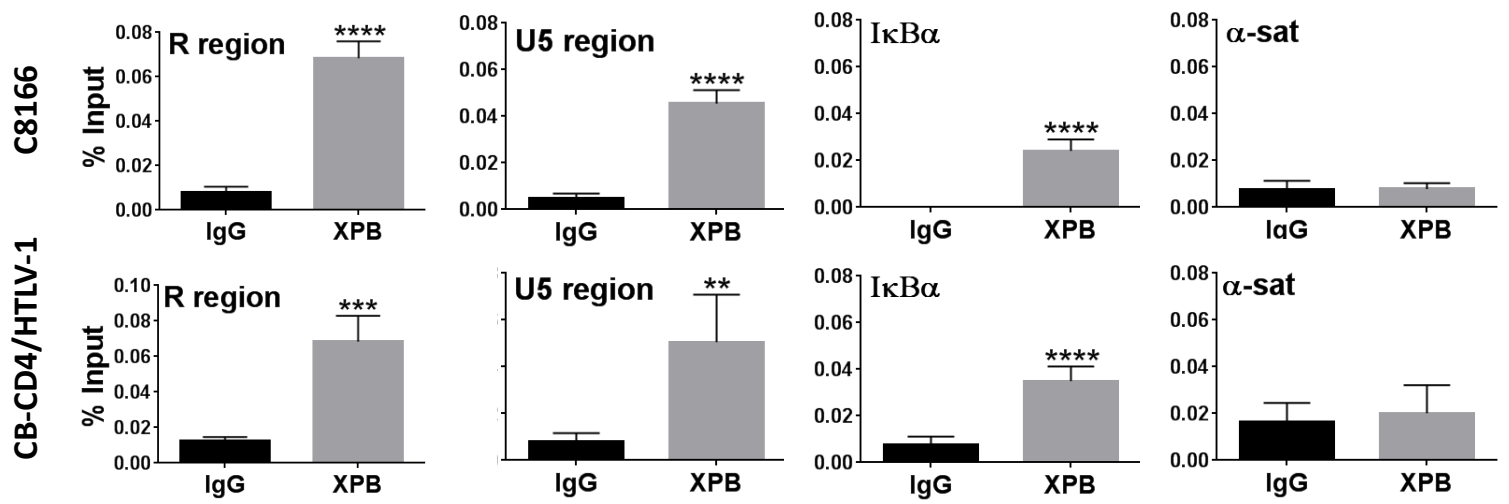


FIGURE 1

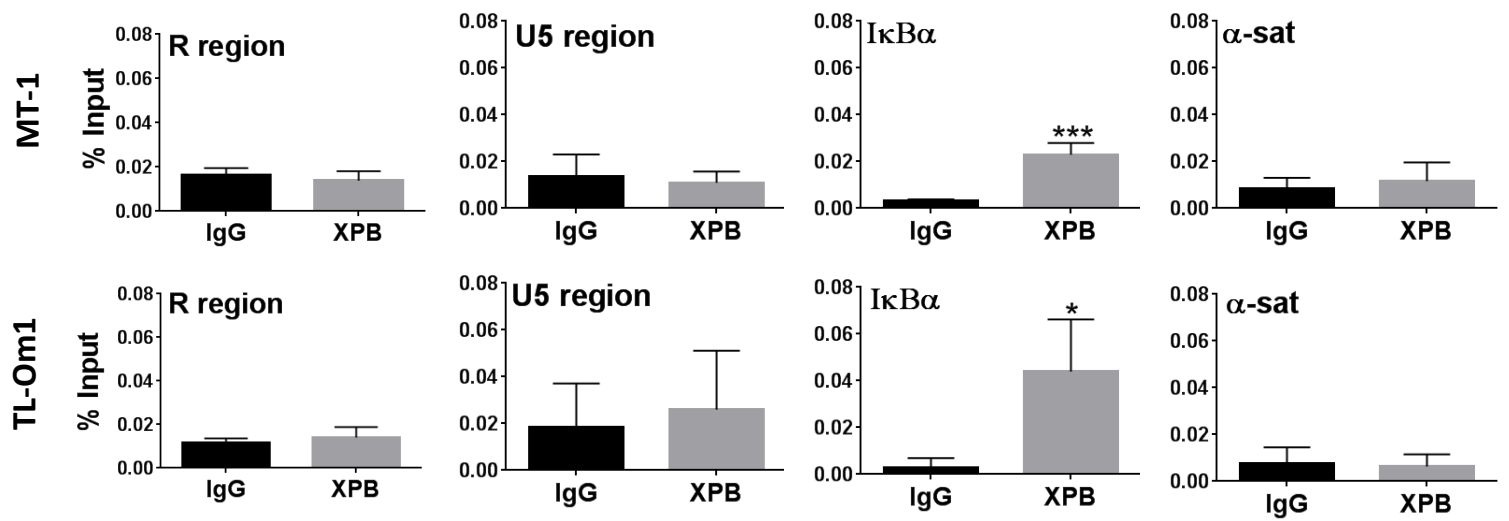
A.

HTLV-1 LTR

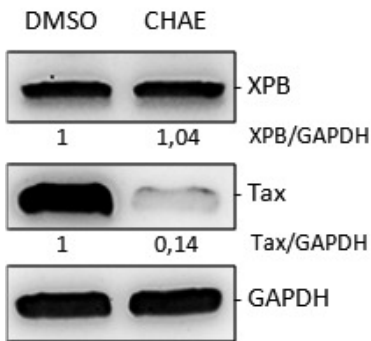


B.

HTLV-1 LTR



C.



D.

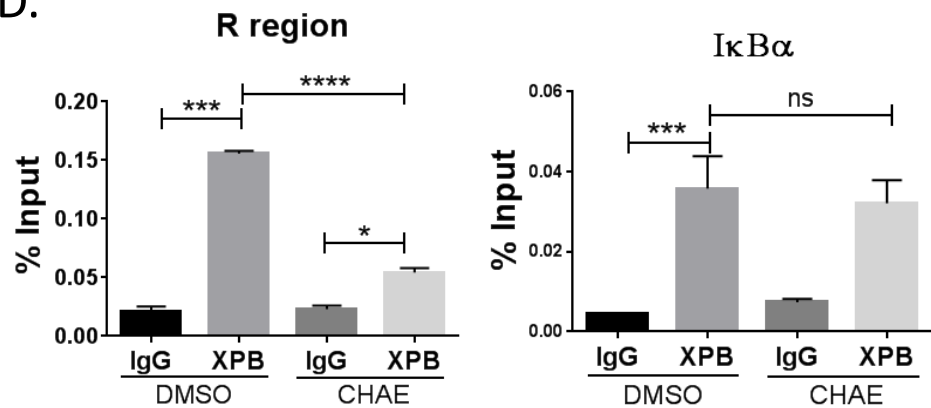


FIGURE 2

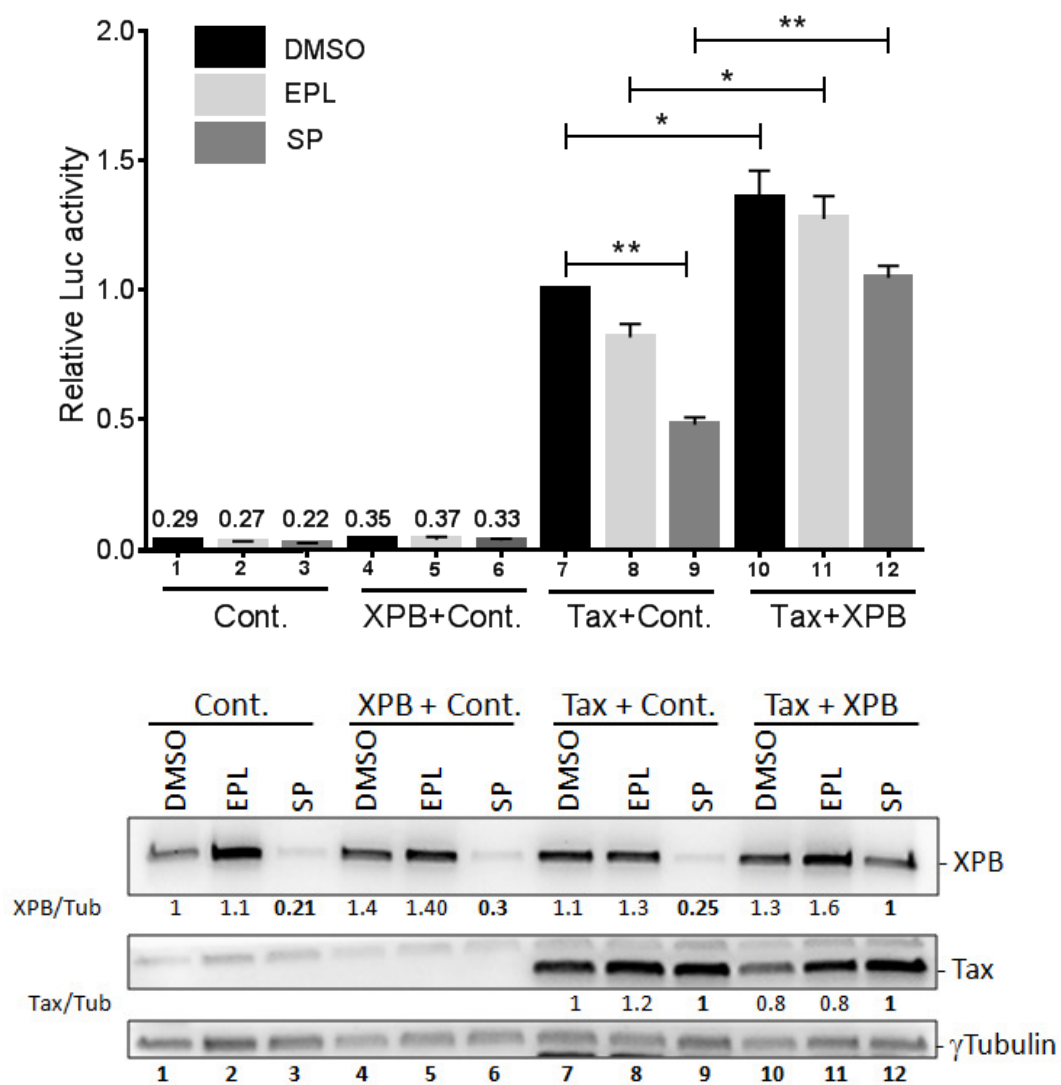


FIGURE 3

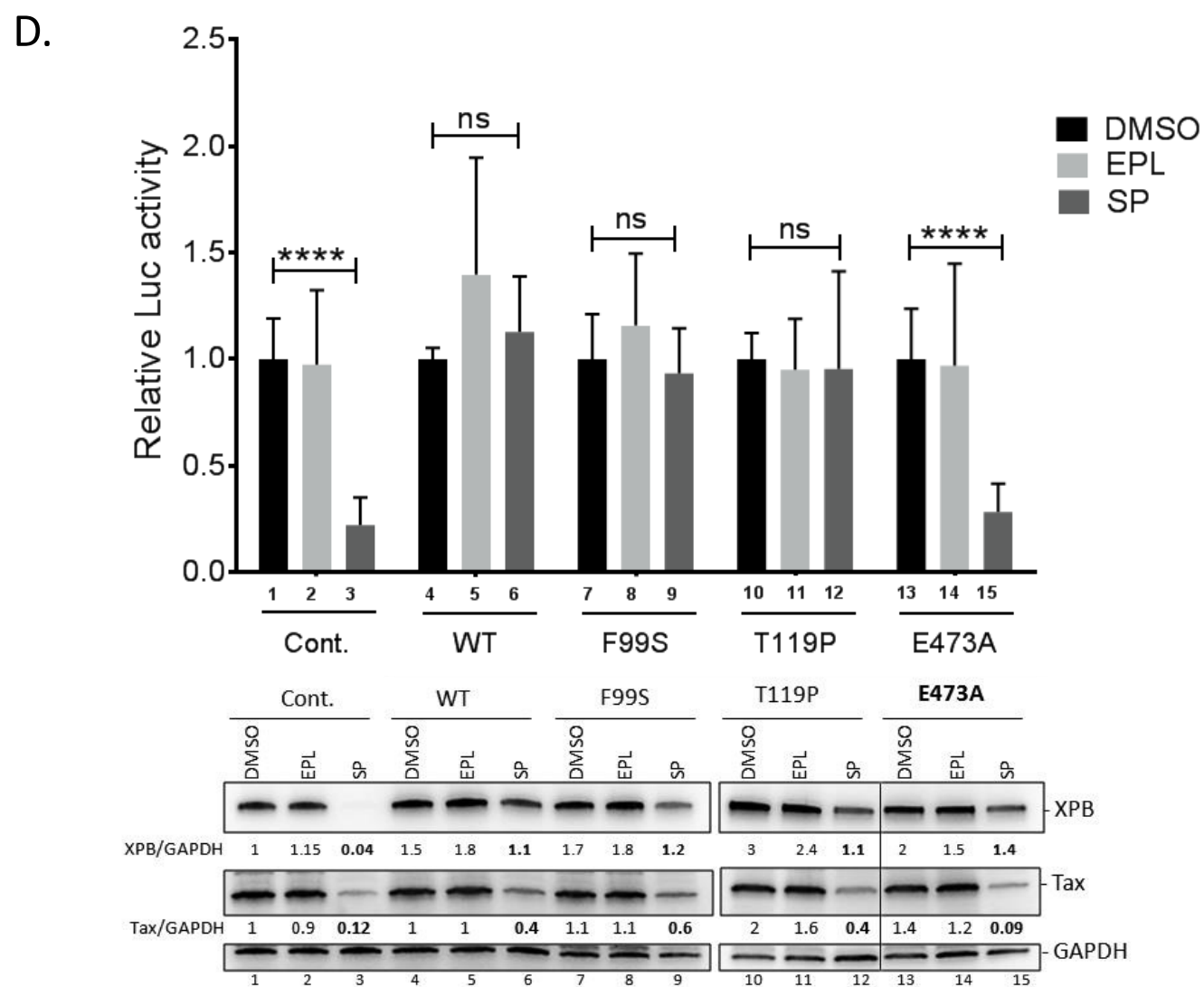
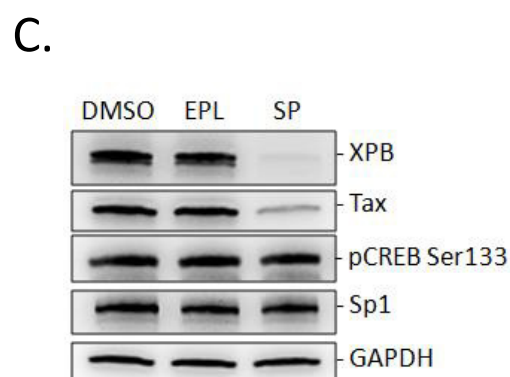
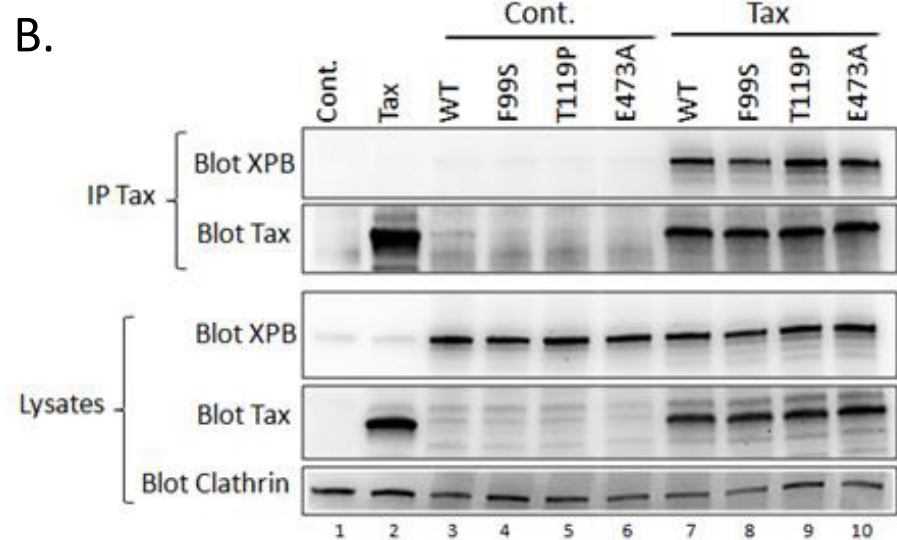
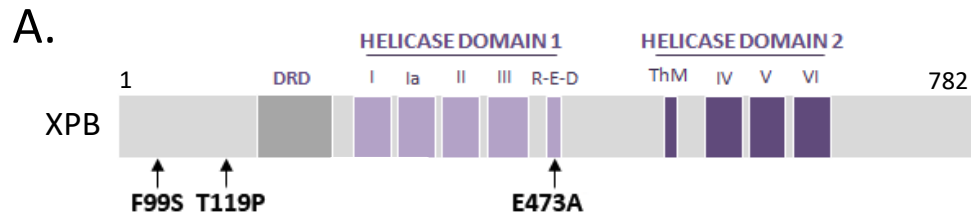


FIGURE 4

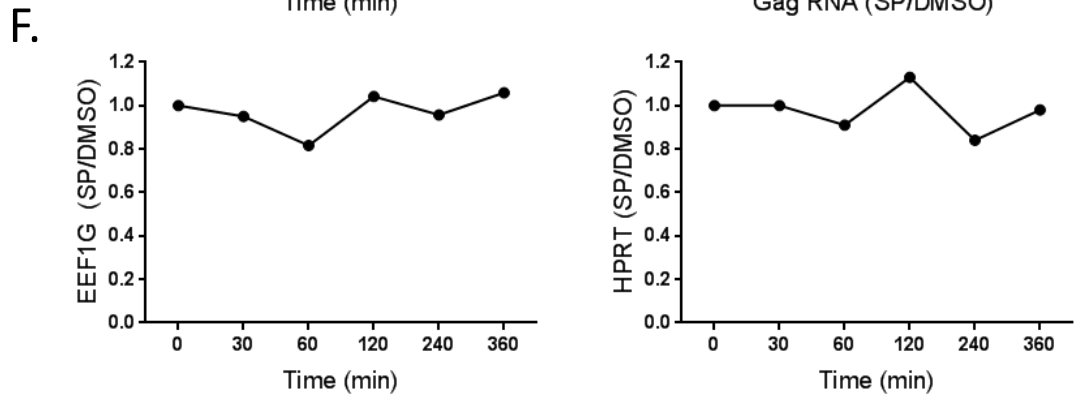
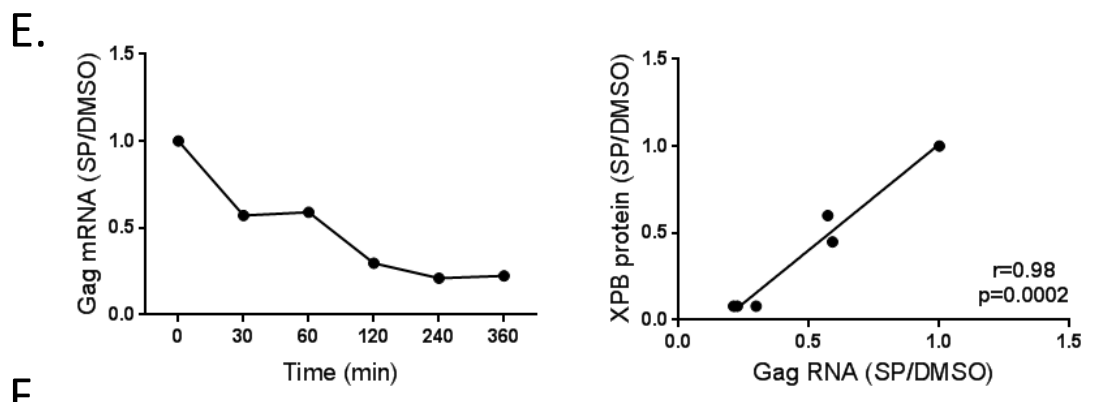
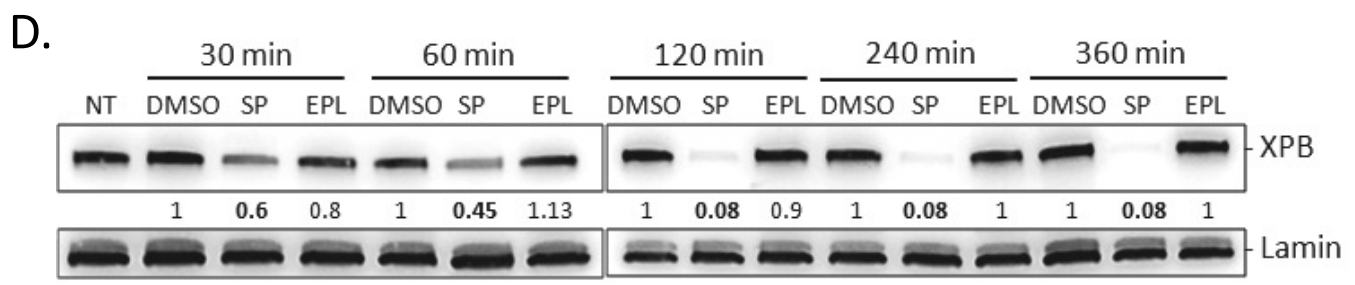
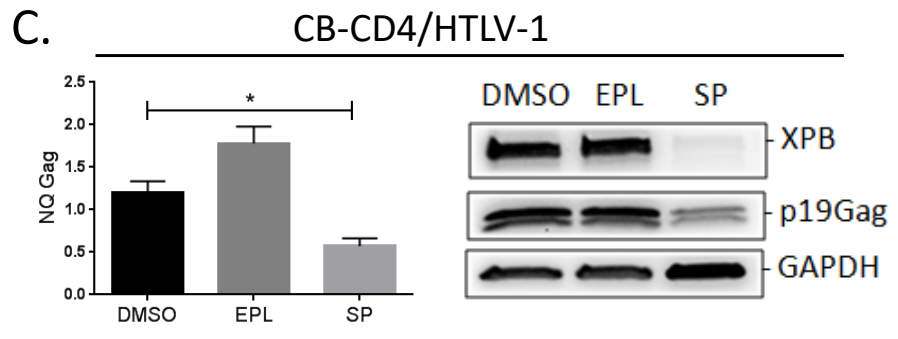
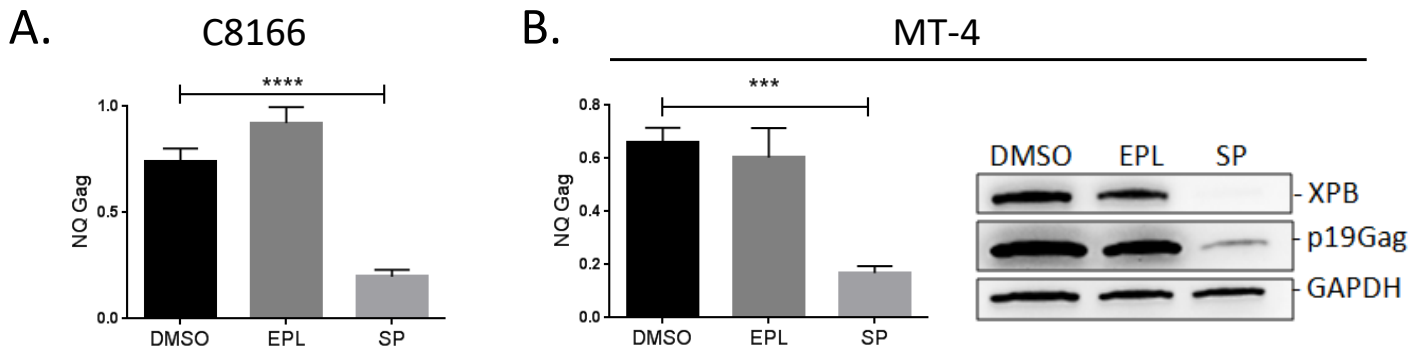


FIGURE 5

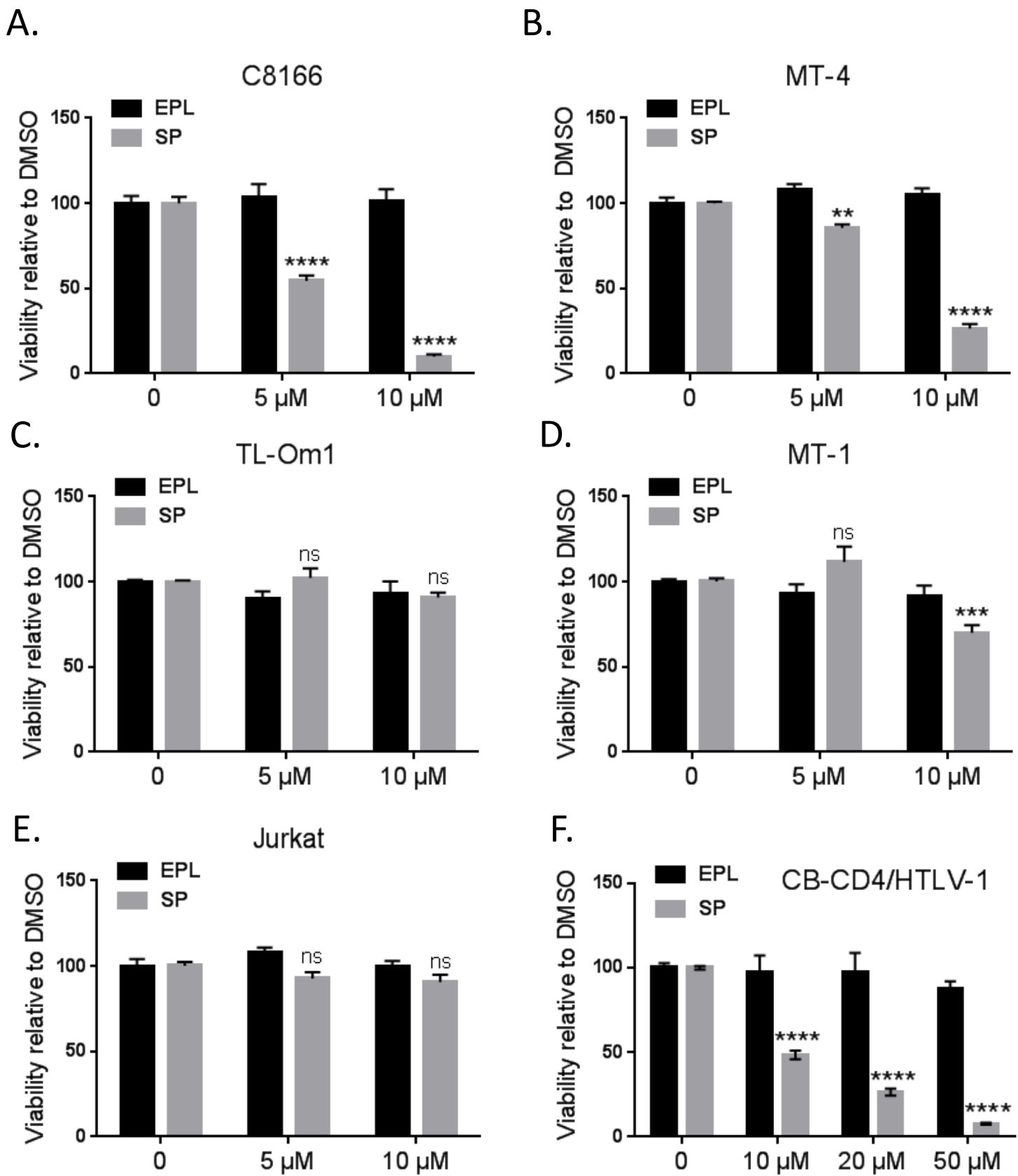


FIGURE 6

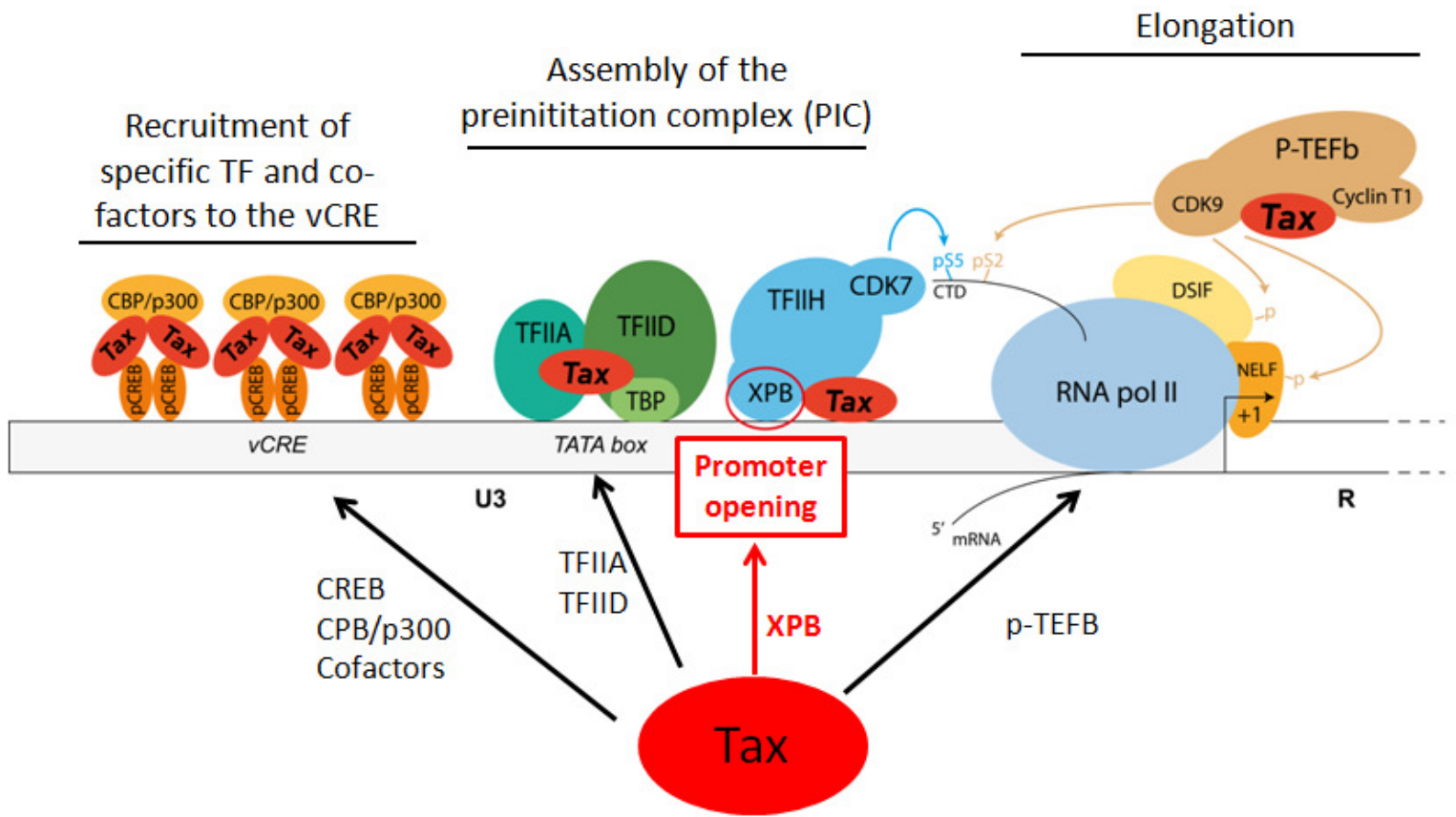


FIGURE 7